Langmuir

ARTICLE

pubs.acs.org/Langmuir

Transformation of ActoHMM Assembly Confined in Cell-Sized Liposome

Kingo Takiguchi,*[,†] Makiko Negishi,[‡,§] Yohko Tanaka-Takiguchi,[†] Michio Homma,[†] and Kenichi Yoshikawa*[,‡]

[†]Division of Biological Science, Graduate School of Science, Nagoya University, Nagoya 464-8602, Japan

[‡]Department of Physics, Graduate School of Science, Kyoto University, Kyoto 606-8502, Japan

Supporting Information

ABSTRACT:

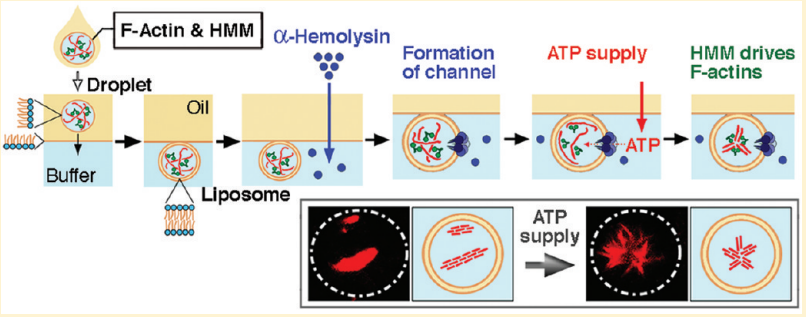

To construct a simple model of a cellular system equipped with motor proteins, cell-sized giant liposomes encapsulating various amounts of actoHMM, the complexes of actin filaments (F-actin) and heavy meromyosin (HMM, an actin-related molecular motor), with a depletion reagent to mimic the crowding effect of inside of living cell, were prepared. We adapted the methodology of the spontaneous transfer of water-in-oil (W/O) droplets through a phospholipid monolayer into the bulk aqueous phase and successfully prepared stable giant liposomes encapsulating the solution with a physiological salt concentration containing the desired concentrations of actoHMM, which had been almost impossible to obtain using currently adapted methodologies such as natural swelling and electro-formation on an electrode. We then examined the effect of ATP on the cytoskeleton components confined in those cell-sized liposomes, because ATP is known to drive the sliding motion for actoHMM. We added α-hemolysin, a bacterial membrane pore-forming toxin, to the bathing solution and obtained liposomes with the protein pores embedded on the bilayer membrane to allow the transfer of ATP inside the liposomes. We show that, by the ATP supply, the actoHMM bundles inside the liposomes exhibit specific changes in spatial distribution, caused by the active sliding between F-actin and HMM. Interestingly, all F-actins localized around the inner periphery of liposomes smaller than a critical size, whereas in the bulk solution and also in larger liposomes, the actin bundles formed aster-like structures under the same conditions.

1. INTRODUCTION

Cytoskeletal assembly of actin filaments (F-actin) plays an essential role in determining the morphology and self-propelling movement of living cells.[1−8] To gain insight into the dynamic behavior of living cells, an artificial cell model (cell-sized giant liposomes with cytoskeletal proteins) has been developed using methodologies such as natural swelling and electro-formation, as a consequence of a reconstituting approach.[9−17] Cell-sized giant liposomes, as well as microcapsules tens of micrometers in diameter, have been actively studied for various applied and fundamental studies in physical, medical, and life sciences because of their simplicity and capability to be observed directly with optical microscopes.[18−20] The dynamic behaviors and changes in the shape of liposomes, which are driven by the assembly of cytoskeletal proteins within them, have been visualized by optical microscopy. Those studies revealed that liposomes are transformed accompanied by the polymerization and/or bundling of actin. However, in living cells, actin undergoes its functions in cooperation with various myosin motor proteins under physiological salt conditions (several millimolar Mg^{2+} and several tens of millimolar K^+ or Na^+). To the best of our knowledge, there has been no report of the successful construction of giant liposomes encapsulating actin, myosin, and their fuel (Mg-ATP) in a physiological condition.

Recently, there have been several attempts to employ water-in-oil (W/O) droplets coated by phospholipids as a precursor of liposomes.[21−30] W/O droplets are easily prepared by emulsifying an aqueous solution together with an oil containing phospholipids. Such a procedure allows the encapsulation of biomolecules at a controlled concentration under any salt strength into cell-sized

Received: November 24, 2010
Revised: August 7, 2011
Published: August 08, 2011

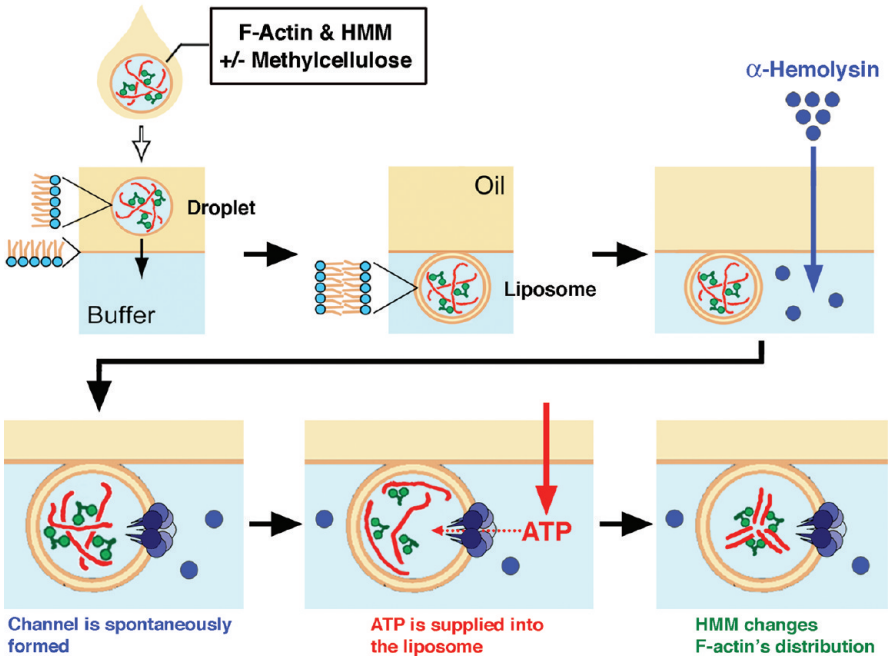

Figure 1. Schematic representation of the experimental procedure used to examine the effect of ATP influx on actoHMM inside cell-sized liposomes. A W/O droplet in the oil phase is transferred into the aqueous phase through the bulk oil/water interface with a phospholipid monolayer (top left to center); F-actin and HMM are illustrated with red and green, respectively. Next, α-hemolysin and/or ATP are added to the aqueous solution. α-Hemolysin forms channels as heptamers cross the lipid bilayer spontaneously. Finally, ATP is supplied into the liposomes from the bulk aqueous phase. Driven by the chemical energy of ATP, HMM moves along F-actins. Thus, changes can be observed for the distribution of proteins through real-time observation. At the individual experimental conditions, we have performed at least in triple independent experimental runs, to confirm the reproducibility.

compartments covered with a monolayer of phospholipids. Consequently, the spontaneous transfer method, which can generate liposomes by transferring phospholipid-coated W/O droplets from a bulk oil phase to a bulk aqueous phase through their interface, has been developed.[24,25,27] By applying that methodology, one can prepare liposomes with sizes of 10−100 μm containing desired amounts of molecules, and we have successfully constructed giant liposomes encapsulating 200 μM F-actin in the presence of 5 mM $MgCl_2$ and 50 mM KCl.[27,31] Note that 200 μM F-actin is comparable to the actin concentration in living cells.[32,33] In practice, this concentration of actin is the upper limit to handle because it is too viscous to be emulsified in the lipid-containing oil to obtain W/O droplets through the pipetting procedure. This method enables us to encapsulate desired amounts of F-actin and HMM inside these giant liposomes.[27] The motor domain of myosins, which is required and sufficient to generate actin-sliding movement, is termed the "head". HMM is a double-headed derivative of conventional myosin (myosin-II) and is able to cross-link F-actins into bundles or gels, and moreover to transform actin bundles or actin gels.[34,35] When F-actin was encapsulated inside the liposomes together with HMM, network structures were generated, whereas F-actin was distributed homogeneously inside the liposomes in the absence of HMM. Thus, cell-sized giant liposomes containing both F-actin and HMM might overcome the first critical step for developing an artificial cell model capable of locomotion or shape change.

An important problem that remains is to construct an open system using closed giant liposomes to continuously control the reaction between F-actin, HMM, and ATP. An approach to supply ATP into our developed system is essential to construct a system consisting of liposomes and cytoskeletal and motor proteins. In this study, we further developed the spontaneous transfer method to overcome this problem. We used α-hemolysin, a bacterial membrane pore-forming toxin, which can spontaneously penetrate a lipid bilayer membrane by self-assembling as a heptamer and can form channels larger than 2 nm in diameter,[23,28,36,37] to introduce ATP inside the liposomes from the bathing solution.[38] In this study, we also examined the effect of intracellular crowding environment by adding methylcellulose with relatively high concentration into the liposome. We adapted methylcellulose because of its bulky structure of hydrophilic property without electronic charge, to mimic the crowding environment. Actually, in a past study, it has been shown that formation of an aster-like assembly of actin bundles with HMM is promoted in a solution with methylcellulose, where the active sliding force generated by HMM plays the essential role under the chemical energy supply by ATP.[34,35]

2. MATERIALS AND METHODS

2.1. Chemicals. 1,2-Dioleoyl-*sn*-glycero-3-phosphatidylcholine (DOPC), 1,2-dipalmitoyl-*sn*-glycero-3-phosphatidylcholine (DPPC), phosphatidylcholine isolated from a native source (egg yolk l-α-phosphatidylcholine, eggPC), and cholesterol were purchased from Sigma (St. Louis, MO) or Avanti Polar Lipids (Alabaster, AL). Mineral oil was purchased from Nacalai Tesque (Kyoto, Japan). Rhodamine-phalloidin (R-415) was purchased from Invitrogen (Carlsbad, CA). Those chemicals were used without further purification. Methylcellulose (1500 cP) was purchased from Wako Pure Chemical (Osaka, Japan) and was dissolved in and dialyzed at least overnight against Milli-Q water to make a 2% stock solution (NaN_3 at 5 mM was added).

2.2. Proteins. Actin and myosin were obtained from rabbit skeletal muscles, and HMM and S-1 (subfragment 1) were obtained by digestion

dx.doi.org/10.1021/la2016287 |*Langmuir* 2011, 27, 11528–11535

of myosin with chymotrypsin as previously detailed.[34,35,39] Actin was polymerized in F-buffer (2 mM Tris-HCl, pH 8.0, 30 mM KCl, and 0.2 mM ATP) and then used for the experiments. To visualize F-actin entrapped within liposomes, rhodamine-phalloidin was added to the actin or actoHMM solution (the molecular ratio against actin monomer was approximately 1/40). α-Hemolysin was purchased from Sigma.

2.3. Preparation and Observation of Liposomes. The preparation and observation of liposomes was performed by the spontaneous transfer method as previously reported.[24,27,31] The observation chamber consisted of a cylindrical hole in a poly(dimethylsiloxane) (PDMS) sheet (ca. 5 mm thick), which was obtained by mixing the base solution and a curing agent of Silpot 184 W/C (Dow Corning Toray, Tokyo, Japan), on a glass microscope slide (0.12−0.17 mm thick).

Briefly, 5 μL of an aqueous solution (buffer A: pH 7.5 with 25 mM imidazol-HCl, 5 mM $MgCl_2$, 50 mM KCl, and 10 mM DTT) containing F-actin or actoHMM was mechanically mixed with 100 μL of oil containing lipids (0.5 or 1.0 mM) to obtain W/O droplets through the pipetting procedure. To obtain actoHMM bundles, the actoHMM solution was gently added to the above solution with methylcellulose at a final concentration of 0.3% (w/v) (the critical overlap concentration c^* is about 0.2%),[34,40,41] and incubated for several minutes.[34,35,42] The methylcellulose allows the crowding condition to form stable bundles of actoHMM. A 5 μL aliquot was then emulsified in the lipid-containing oil to form W/O droplets as described above. The oil containing the W/O droplets was then situated on an oil phase (10 μL, containing 0.5 or 1.0 mM lipids) that had been placed above an aqueous phase (10 μL, buffer A, up to twice the concentration of buffer A or buffer A with sucrose, to regulate the osmolarity). The lipid compositions used were eggPC, DOPC, or DOPC/DPPC/cholesterol (4:4:2, molar ratio). We selected lipid concentrations and compositions needed to obtain giant liposomes with sufficient stability. We have confirmed that small changes in lipid composition do not cause any critical effect in the present study.

The prepared solution with bulk two-phase was then held steady, during which time the W/O droplets gradually fell onto the oil/water interface due to gravity. Interestingly, the W/O droplets then spontaneously transferred through the interface into the aqueous phase while keeping their spherical shape, as indicated schematically in Figure 1. Under our experimental conditions, most liposomes are anchored onto the interface.[27] Although it is possible to transfer the liposomes into the bulk aqueous phase by use of centrifugation, we performed the observation on the liposomes anchored to the interface. By adapting such method on the observation, it becomes possible to monitor the individual droplets/liposomes for the full process of the transfer. In addition to this, we could capture the better microscopic image by focusing the liposome attached at the interface than those of the liposome existing freely in the bulk aqueous solution.

Observations were performed using a Zeiss Axiovert 100 inverted microscope equipped with a LSM 510 module for confocal microscopy. Unless noted otherwise, the samples for observation were prepared, and the observations were performed at 25 °C. The recorded images were analyzed using ImageJ software.

2.4. Supplying ATP into actoHMM-Entrapping Liposomes through Embedded α-Hemolysin. After the formation of actoHMM-containing liposomes, 5 μL of α-hemolysin solution with/without 10 mM ATP (the final concentration of α-hemolysin was 12.5 μg/mL) was added to the aqueous phase using a narrow pipet tip (Catalogue No. 010, Quality Scientific Plastics, Kansas City, KS) (Figure 1). Once the α-hemolysin interacts with a lipid bilayer membrane, it spontaneously penetrates the membrane and forms heptamers to open channels with about 2 nm diameters.[23,28,36−38] Although the kinetic process has not been fully clarified yet, α-hemolysin has been utilized as a powerful tool to construct open systems consisting of membrane vesicles. The diameter of each membrane channel is suitable to supply ATP into the actoHMM-containing liposomes because the size is large enough to allow the transfer of ATP (its size is much less than 1 nm) from the external solution but is too small to allow the encapsulated actin and HMM proteins (both monomer actin and HMM are larger than 5 nm) to leak out to the external solution.

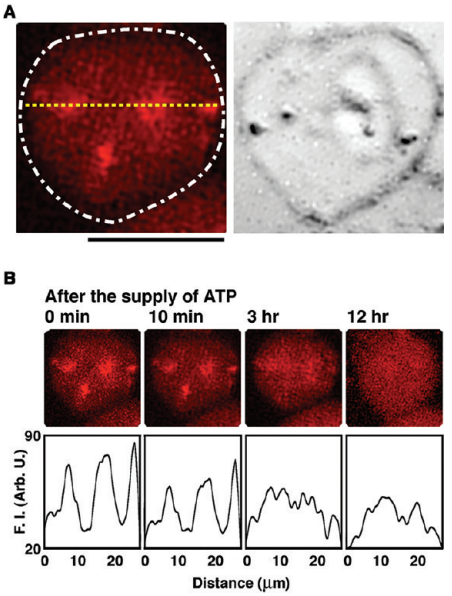

Figure 2. Fluorescence microscopic observations on the time-dependent changes in the distribution of actoHMM after the addition of ATP to the liposomes. (A) Left: Confocal fluorescence microscopic image of an actoHMM-encapsulating giant liposome with a DOPC bilayer membrane produced by the spontaneous transfer method. The concentrations of encapsulated F-actin and HMM are 50 and 5.0 μM, respectively. The distribution of F-actin, which is labeled with rhodamine-phalloidin, is shown. The white dashed line indicates the shape of the liposome observed in a transmission image. Right: The transmission image. The small spherical objects situated on the surfaces of liposomes in the transmission images are attributed to oil droplets in the water phase.[24] Bar = 20 μm. (B) Top: Images showing the disassembly process of cross-linked F-actins that have formed by the rigor complex with HMM inside the liposome shown in (A). Time after the addition of ATP induced by α-hemolysin is indicated at the top of each panel. Bottom: Relative fluorescence intensity profiles of the top panels at the position indicated by the yellow dotted line in (A). F.I. = fluorescence intensity. The sample was observed for 3 h at 25 °C, and then left for 12 h at 4 °C. The picture on the right is the observation after the sample was adjusted back to 25 °C. The probability of disassembly of cross-linked F-actins was found to be 95% among the observed 200 liposomes.

3. RESULTS AND DISCUSSION

3.1. ATP-Driven Distribution Changes of actoHMM in Giant Liposomes. Figure 2A exemplifies a fluorescence microscopic image of a giant liposome encapsulating F-actin and HMM in the presence of $MgCl_2$. Robust actin bundles and networks are observed, due to the strong and tight binding between the motor head domain of each HMM and F-actin in the absence of ATP (rigor state).[27,31] We have confirmed the appearance of similar assemblies of F-actin in bulk aqueous solution.

Figure 2B shows the time-dependent change on the spatial distribution of actoHMM after the supply of ATP. We expect that the cross-linking of F-actins by the double-headed HMM is released and the sliding motion of F-actins is induced by the

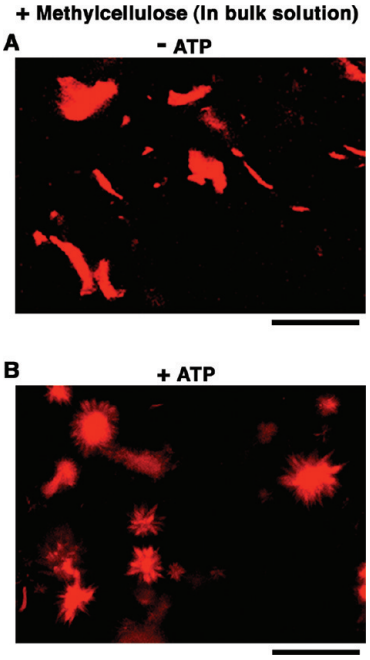

Figure 3. Changes in the shape of actoHMM bundles induced by ATP in the bulk solution with 0.3% methylcellulose as observed by confocal fluorescence microscopy, where F-actin is labeled with rhodamine-phalloidin. (A) Without ATP, bundles have the typical structure. For a reference, length distribution of F-actin within actoHMM bundles is shown in Figure S4. (B) 30 min after the addition of 10 mM ATP, the formation of aster-like structures is noted. The transformation of actoHMM bundles in bulk solutions is not affected by the addition of α-hemolysin. Bars indicate 100 μm.

addition of ATP, due to the myosin heads escaping from the rigor state and turning into the active state. During the incubation, actin bundles and their network gradually dissolved into a dispersed state (Figures 2B and S1). After overnight incubation, the F-actins were redistributed inside the liposomes almost uniformly. We have demonstrated that, under such conditions, ATP is exhausted after the overnight incubation.[34,39] Thus, the results shown in Figure 2B imply the dissolution of actoHMM into a dispersed state while F-actin remains stable.

To further clarify this mechanism, we performed similar experiments under different conditions: (1) without the addition of ATP, (2) without the addition of α-hemolysin, and (3) without the addition of ATP and α-hemolysin. No visible change in the distribution of F-actin or actoHMM ever appeared under any of those three conditions. In addition, we carried out a similar experiment without actoHMM, that is, only in the presence of F-actin, and confirmed that F-actin alone does not exhibit any notable change inside the liposomes.

We then examined the effects of structural differences in the motor proteins, by replacing HMM with S-1; that is, the double-headed protein was changed to a single-headed protein (Figure S2). F-actin inside the liposomes remained in a homogeneous distribution, even under conditions where excess molar S-1 was coencapsulated.[27] The results of these experiments indicate that the cross-linking of F-actins by double-headed HMM is the motive force for the organization of bundles and networks of actin, in accordance with the past studies.[1−8] We have confirmed similar trends inside a confined environment of giant liposome, except for the significant surface effect as shown later in Figure 4.

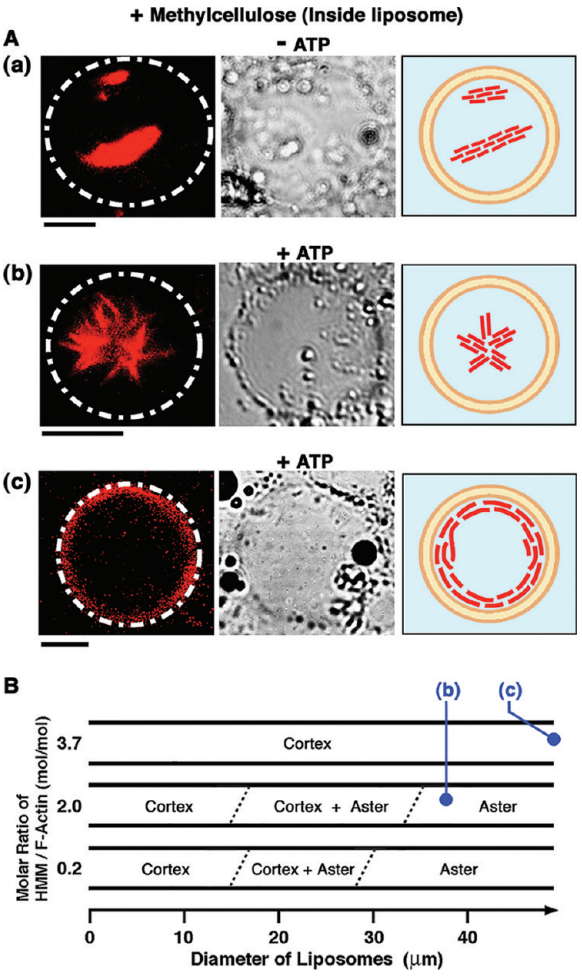

Figure 4. (A) Transformation of actoHMM in a giant liposome caused by the ATP supply, according to the experimental procedure shown in Figure 1. Left: The fluorescence microscopic images showing the distribution of F-actin. The white dashed lines indicate the shapes of liposomes observed in the transmission images. Center: The transmission images. The small spherical objects situated on the surfaces of liposomes are attributed to oil droplets in the water phase.[24] Right: The pictures showing schematic representations of the distribution and shape of actoHMM. A 0.3% methylcellulose solution was used. (a) Bundles of actoHMM inside the liposome without ATP ("− ATP"). The concentrations of F-actin and HMM were 10 and 20 μM, respectively. (b) Formation of the aster-like assembly caused by ATP supplied from the outer solution through the channel created by α-hemolysin ("+ ATP"). The concentrations of F-actin and HMM are 10 and 20 μM, respectively. This image was captured 15 min after the ATP supply. (c) Formation of the cortex structure by actoHMM in a liposome at a relatively high ratio of HMM with respect to F-actin; F-actin and HMM concentrations were 10 and 37 μM, respectively. The image was captured 30 min after the ATP supply. Bars indicate 20 μm. The lipid composition was DOPC/DPPC/cholesterol. (B) Diagram of the morphology of actoHMM inside the liposome observed after the ATP supply, as functions of liposomal size and the molar ratio of HMM and F-actin, at a fixed F-actin concentration of 10 μM. For each condition shown in the diagram, 20−40 liposomes were observed and counted. The images of (b) and (c) in (A) are consistent with the symbols in (B).

3.2. Transformation of actoHMM Bundles Inside Liposomes under Crowding Conditions. Figure 3 shows the morphologies of actoHMM bundles without ("− ATP") or with

dx.doi.org/10.1021/la2016287 |*Langmuir* 2011, 27, 11528–11535

ATP ("+ ATP"), generated in a crowding solution with methylcellulose, where the concentrations of F-actin and HMM are 10 and 20 μM, respectively. Bundles were observed in the bulk solution (10 μL of buffer A) after pipetting in the same way as to form W/O droplets containing bundles (Figure 3A). After that, an ATP solution (5 μL of buffer A, that contained a final concentration of 10 mM ATP) was added, and the sample was observed about 30 min later (Figure 3B). From in vitro studies, it has been established that actoHMM, as well as F-actin, forms bundle structures in the presence of relatively large amounts of inert high polymers, such as methylcellulose or PEG.[42] In those bundles, a large number of F-actins were closely aligned in parallel with overlaps. Such an effect in the crowding environment has been interpreted in terms of the depletion effect.[42,43] Such bundles of actoHMM or F-actin are nonpolar.[34,35,42] Together with the generation of the bundles, these proteins cause spindle-like structures as exemplified in Figure 3A. The complexes of HMM and F-actin thus formed in the crowding condition then were transformed following the addition of Mg-ATP, due to the sliding motion between F-actins and HMM.[34,35] Successively, each bundle showed contraction, elongation, bending, or twisting. Following these shape changes or active motion, each bundle tended to split longitudinally into several bundles in a stepwise manner, while the newly formed bundles remained associated with either end. The product, an aster-like assembly of actoHMM (Figure 3B), was stable; that is, the individual bundles never contracted upon the further addition of ATP. It is to be noted that similar aster-like assemblies of F-actin are found in living cells.[44−46]

Figure 4A(a) shows giant liposomes encapsulating actoHMM bundles together with methylcellulose at the concentration sufficient for maintaining bundle formation. It should be noted that it had been almost impossible to prepare liposomes containing such highly concentrated proteins and inert polymer.[27,31]

Figure 4A(b) and (c) shows the morphology and distribution of actoHMM assemblies inside liposomes after the supply of ATP through the pores of α-hemolysin. In some of the liposomes, we observed the formation of aster-like structure (Figure 4A(b)), the shape of which was essentially the same as that formed through the contraction of actin bundle in the bulk solution.[34,35] Interestingly, however, in most liposomes, actoHMM bundles were redistributed to the periphery of the inner surface, forming so-called cortexes (Figure 4A(c)). Almost all of the encapsulated bundles were transformed either to asters or to cortexes. One should note that during these experiments, the morphology of the giant liposomes did not show any notable changes. Furthermore, we could also confirm that the changes in shape or distribution of actoHMM were not generated in the absence of α-hemolysin and/or ATP.

Figure 4B shows that liposomes entrapping asters were larger than those entrapping cortexes. We investigated the dependence of the actoHMM morphologies on HMM concentration, while keeping the concentration of F-actin constant at 10 μM. When the HMM concentration was 2.0 μM, all encapsulated bundles were transformed to asters when the liposome diameter was more than 30 μm, whereas they changed to cortexes when the liposome diameter was less than 15 μm. By analyzing the statistical average, asters were found in 14% of the liposomes, which was smaller than the fraction of asters, 44%, in bulk solution under identical condition. When the HMM concentration was increased to 20 μM, almost all of encapsulated bundles were transformed as well either to asters or to cortexes. However,

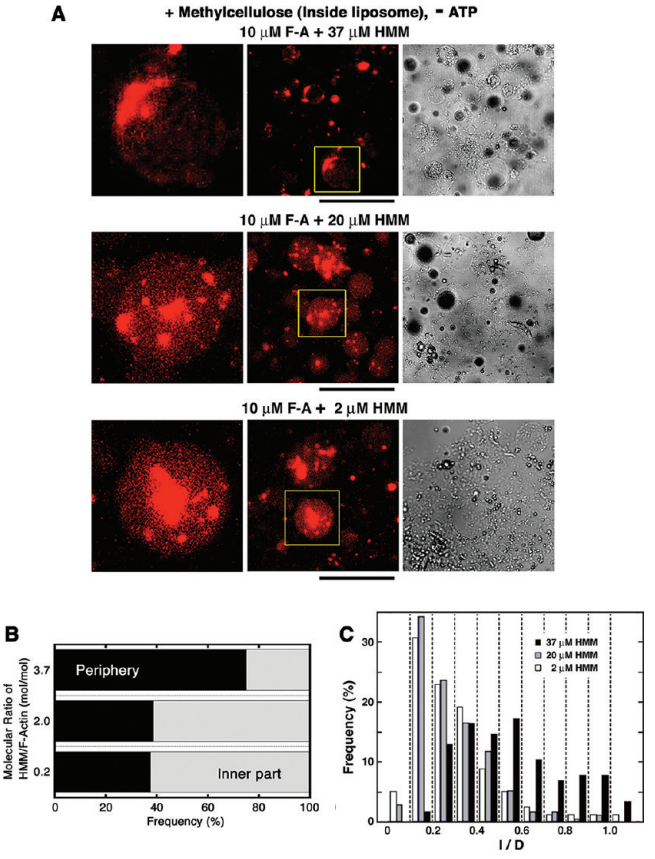

Figure 5. The encapsulated actoHMM bundles inside liposomes before the ATP supply. (A) Representative images of encapsulated actoHMM bundles inside liposomes before the addition of ATP (center, fluorescence; right, transmission). Liposomes encapsulate 10 μM F-actin. The concentration of coencapsulated HMM is 37 (upper), 20 (middle), or 2.0 μM (bottom), as indicated at the top of each panel. A 0.3% methylcellulose solution was used. Each frame on the left is an enlarged image of a representative liposome indicated by the yellow boxes in the center. Bars indicate 100 μm. The lipid composition was DOPC/DPPC/cholesterol. In the transmission images, the black shadows are W/O droplets floating nearby.[24] (B) Diagram of the localization of encapsulated actoHMM bundles inside liposomes observed before the ATP supply, as functions of the molar ratio of HMM and F-actin, at a fixed F-actin concentration of 10 μM. For the conditions at 2.0, 20, and 37 μM of HMM in the diagram, 115, 420, and 140 bundles were counted in the observation, respectively. (C) The ratio of the bundle length to the diameter of the encapsulating liposome (l/D) was measured. The length of the encapsulated actoHMM bundle was measured from their fluorescence images, and the diameter of the encapsulating liposome was obtained from their transmission images by use of ImageJ software, respectively. Concentrations of F-actin and HMM are 10 μM, and 2.0 (open, n = 78), 20 (gray, n = 169), or 37 μM (filled, n = 115), respectively. It should be noted that there are few bundles with an l/D of 1.0−1.1, presumably due to measurement error.

the critical liposome diameter, to ensure the formation of only asters inside liposomes, was increased to 35 μm. This resulted in a decrease in the fraction of asters to 9.7% observed in the liposomes, while in bulk solution under identical condition the fraction of asters was increased to 89%. When the HMM concentration was further increased to 37 μM, a condition should be the most favorable among those experimented here for the formation of asters at least in bulk solution, because actin bundles tend to be transformed to asters more with increases in

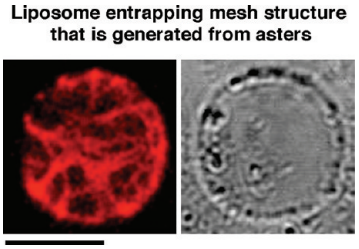

Figure 6. Mesh structure inside cell-sized liposomes with actoHMM. The aster, which was formed in the bulk solution, was suspended and then entrapped in the giant liposome by the spontaneous transfer method (left, fluorescence; right, transmission). The lipid composition was DOPC/DPPC/cholesterol. The concentrations of F-actin and HMM are 10 and 20 μM, respectively. A 0.3% methylcellulose solution was used. Bar indicates 20 μm. Methylcellulose-formed actoHMM bundles are transformed to asters in the bulk solution by the addition of ATP. The asters are then encapsulated into cell-sized giant liposomes by the spontaneous transfer method using the pipetting procedure. By the suspension, the asters change in the mesh. The small spherical objects situated on the surfaces of liposomes in the transmission images are oil droplets in the water phase.[24] It should be noted that the encapsulated mesh is not transformed to an aster or situated on the inner surface periphery even after the addition of both α-hemolysin and ATP (Figure S3). The probability of the mesh generated inside was 75% among 100 liposomes.

the molar ratio of HMM to actin.[35] In fact, in that condition in the bulk solution, all bundles were transformed to asters after the addition of ATP. Inside the liposomes, however, no asters were formed during the entire observation period. In all liposomes, cortex formation was observed, regardless of the liposomal size.

To gain insight into the mechanism for this, we examined the initial state, and thus the distribution and length of encapsulated actoHMM bundles before the ATP supply (Figure 5). Figure 5B shows that the encapsulated actoHMM bundles tended to localize near the inner periphery of each liposome before the ATP supply, as the HMM concentration increased. When the mixing molar ratio was 0.2 or 2.0 (HMM/F-actin), the bundles randomly distributed within the liposomes. However, when the mixing molar ratio was 3.7, where the HMM concentration was far above the maximum binding amount, the bundles tended to localize on the surface. The ratio between the characteristic length of an elastic rod-like structure l_{rod} and the diameter of a spherical space D_{space} is one of the dominant factors that decides the distribution of rod-like elastic structures in a spherical space.[47,48] When $l_{rod} \approx D_{space}$, the rod-like elastic structure tends to localize with bending on the surface of the space.[47,48] Figure 5C indicates the ratio between the length of actoHMM bundles encapsulated and the diameter of the encapsulating liposomes, corresponding to l_{rod}/D_{space}. When the mixing molar ratio of HMM/F-actin was 3.7, the ratio l_{rod}/D_{space} was larger than those for 0.2 and 2.0 of HMM/F-actin. Especially in our experimental situation, liposomes are kept to attach on the water/oil interface. Therefore, the characteristic scale for the depth direction is smaller than the diameter of the liposome, and thus the confinement effect becomes greater. HMM is a cross-linker between F-actins in the absence of ATP as described above, and also it may act as a depleting agent in addition to methylcellulose. These HMM features may make the encapsulated actoHMM bundles longer, when the HMM concentration is far above the maximum binding amount of actins. The nature of the myosin (as well as HMM) adsorbing on any surface is another factor for the actoHMM bundles to localize on the surface in the 3.7 HMM/F-actin mixture.[49] It may be of scientific importance to extend the study in cell-sized phospholipid vesicles entrapping high concentrations of biopolymers and to explore the effect of compartment as exemplified in Figure 6.

The dynamic assembly of actin bundles by the molecular motor-induced active sliding is affected strongly by the geometrical confinement. The buckling of actin filaments during the process forms a cortex structure, but not an aster.[50,51] Therefore, it is reasonable to conclude that the cortex is produced in smaller liposomes or in liposomes where the actoHMM bundles are localized on the surface.

Transformations of the encapsulated actoHMM assembly observed after the ATP supply were quite different between the presence and absence of methylcellulose. In the absence of the depletion agent, dispersion of actin bundles took place similarly to that in the bulk solution, even under the confined environment (Figure 2). On the other hand, in the presence of methylcellulose, formation of the cortex newly was noted, in addition to the aster structure that existed in the control bulk solution (Figure 4). The difference is, thus, attributed to the effect of crowding condition under relatively high concentration of methylcellulose in the liposome. This suggests that crowding condition will contribute to the reactions between the polymers, such as cytoskeletons and molecular motors, which are taking place in living cells.

3.3. Formation of Mesh Structures Inside Cell-Sized Liposomes with actoHMM. Figure 6 shows a cell-sized giant liposome entrapping an actoHMM mesh inside. The mesh was generated from many asters by the pipetting procedure in bulk. The product, such as an aster, which is made by the transformation of a methylcellulose-formed actoHMM bundle, never changed the shape with the following addition of ATP, because F-actins in each bundle are sorted out according to their polarity during the transformation.[34,35] Thus, the actoHMM mesh obtained by the suspension of asters is rather stable and retains its structure inside liposomes, even after the ATP supply (Figure S3).

This indicates the successful preparation of a stable mesh-like structure in a liposome by adopting the confinement effects of the elasticity of an aster-like structure. Living cells utilize dynamic cytoskeletal system to propel their own bodies and also to maintain three-dimensional morphology including inner arrangement. The results shown in Figure 4 reveal the dynamic structural change of nonpolar actoHMM bundles mediated by the ATP energy supply. On the other hand, Figure 6 demonstrates the generation of a specific stable structure inside a cell-sized closed space.

3.4. Applications of the Experimental System Developed in This Study Using the Spontaneous Transfer. To study the confinement effect, it would be interesting to examine how the stability of the aster and cortex states is dependent on the size of the confined space, whereas, at present, it is still difficult to encapsulate actoHMM assembly with the desired size into liposome in a selective manner, because sample solution has to be emulsified in the oil through the pipetting procedure to obtain droplet. To characterize the actoHMM structure formed inside cell-sized liposomes in comparison with actomyosin structures actually existing in living cells, evaluation of the physical properties of the encapsulated actoHMM bundles, such as asters and cortex, in terms of distribution of length (Figure S4), polarity, and packing of F-actins is necessary. Unfortunately, quantitative

analysis on the aster and cortex formed inside liposomes was rather difficult, due to their fragility. In addition, it is necessary to calibrate the ratio l_{rod}/D_{space} through time before and after the ATP supply. However, the interface between oil and aqueous phases was disturbed, and the formed liposomes were driven by the flow as the result of the procedure of the addition of α-hemolysin and ATP to the lower aqueous phase. Thus, under the present experimental situation, it is almost impossible to evaluate the time-dependence of the ratio. To overcome these difficulties, improvement on the experimental procedure would be necessary as the future extension.

Nevertheless, this study demonstrate the marked difference on the structure of actoHMM system in a closed cell-sized space from that in the bulk solution, particularly in the coexistence of highly concentrated hydrophilic polymer, suggesting the important role of confined environment and crowding condition for biological phenomena. The results reported in this study should help to find clues for deploying new reactions to adopt biological phenomena, which would be useful for chemical, pharmaceutical, and engineering uses.

The construction of artificial cell models would be expected to bring significant benefits in various fields not only biology but also from chemistry to physics. The studies with giant liposomes allow one to mimic certain aspects of living cells and to gain deeper insight on the dynamics of life, such as gene expression and/or protein synthesis.[38,52,53] An actual living cell is a highly complicated dynamic system with a large number of components, and studies to construct cell model seem to remain in a primitive stage. For example, to the best of our knowledge, no one has previously succeeded in the reconstruction of active interaction between cytoskeletons and molecular motors inside giant liposomes. Therefore, the results, together with the methodology, reported in this study are expected to play the role as a milestone toward the successful construction of an artificial cell model capable of movement.

Still, however, any remarkable movement or shape change of these giant liposomes has not yet been observed. In our system, to realize spontaneous motion by mimicking living cells, the following parameters should be resolved. (i) In living cells, a number of actin-associating proteins are involved in determining their morphology and motility. Many of those proteins are localized within or beneath the cellular membranes. Therefore, other factors, for example, protein cross-linkers between F-actin and the membrane as well as between F-actins, should be required for liposomal morphogenesis or movement.[54] (ii) It has been well-known that actin dynamics are essential for cell morphology and motility. In addition, it has been reported that actin dynamics are affected by the surface under crowding conditions.[55] Therefore, factors such as proteins, which regulate actin assembly or disassembly, have to be added to the system and their potential directly tested in vitro.[33,56,57] Some regulators of actin dynamics may also serve as protein cross-linkers. In relation to this, it is known that α-actinin or filamin are proteins that are involved in actin-cross-linking, and that Arp2/3 complex, WASP (or WAVE), formin, ADF/cofilin, or profilin are proteins that are involved in actin dynamics.[58] As for future research, it may be interesting to examine the actual role of these biochemical species, by utilizing the experimental system reported herein. As the next step, we expect that the regulation of the size of bundles formed inside the liposome will become possible by utilizing the natural actin effecters and/or depletion reagents. From such an advanced study, we may obtain deeper insight on the relationship between the critical liposome size for the cortex formation and the encapsulated bundle size. (iii) In this study, to simplify the system, we utilized HMM as a motor. However, over 20 classes of myosins have been identified, and some of them possess a membrane-binding ability.[59] They have been regarded as either membrane cargo transporters or membrane morphology regulators. However, their precise roles and how they share those roles in vivo have remained unclear. Thus, those native myosin motors should be used and tested instead of HMM. So far, studies for the mechanism of actin-regulating proteins and myosins have been restricted to those based on an analytical approach. We have expectations that our model system based on a reconstituting approach will overcome those limitations and will help to answer important questions. (iv) In this Article, we used only limited lipids, mainly native or synthetic PC, as components of the liposome membrane. Biological membranes, however, consist of various types of lipid molecules, and, moreover, it has been reported that acidic phospholipids such as phosphatidylserine or phosphoinositides are important for many actin-binding proteins. Thus, the lipid composition needs to be considered as well.

The spontaneous transfer method is a very convenient approach to supply cell-sized giant liposomes that contain desired amounts of complex protein systems and that consist of various combinations of lipids.[27,31] The experimental system developed in this study is expected to serve as a powerful tool for unveiling mechanisms that maintain membrane morphology and/or movement in living cells.

4. CONCLUSIONS

In this study, using α-hemolysin to generate pores, we successfully supplied ATP inside cell-sized giant liposomes encapsulating actoHMM, which were obtained by the spontaneous transfer method. Accompanied by the ATP supply, (i) self-organized actin networks, which are formed from the encapsulated actoHMM, gradually dispersed into individual F-actins within the liposomes, and (ii) actoHMM bundles, which had been formed with methylcellulose (a depletion reagent) and subsequently encapsulated into liposomes, changed shape and/or distribution in a characteristic manner. The changes observed in the encapsulated actoHMM can be attributed to the revelation of F-actins from cross-linking by strong binding with double-headed HMM and the active sliding between F-actins and HMM, because both ATP, the fuel for HMM, and α-hemolysin, which creates the membrane channel to introduce ATP into liposomes, are required. Moreover, remarkable differences in the behavior of F-actins were found; that is, inside liposomes, almost all F-actins were situated around their inner periphery, whereas, in the bulk solution, actin bundles form aster-like structures.

■ ASSOCIATED CONTENT

Supporting Information. Figures S1−S4. This material is available free of charge via the Internet at http://pubs.acs.org.

■ AUTHOR INFORMATION

Corresponding Author

*Phone: +81-52-789-2993 (K.T.); +81-75-753-3812 (K.Y.). Fax: +81-52-789-3001 (K.T.); +81-75-753-3779 (K.Y.). E-mail: j46037a@nucc.cc.nagoya-u.ac.jp (K.T.); yoshikaw@scphys.kyoto-u.ac.jp (K.Y.).

Present Addresses
[§]Department of Basic Science, Graduate School of Arts and Sciences, The University of Tokyo, Tokyo 153-8902, Japan.

■ ACKNOWLEDGMENT

This work was supported by the Japan Society for the Promotion of Science (JSPS) under a Grant-in-Aid for Creative Scientific Research (Project No. 18GS0421) and by the Ministry of Education, Culture, Sports, Science and Technology of Japan (MEXT) under a Grant-in-Aid for Scientific Research on Priority Area, "System Cell Engineering by Multi-Scale Manipulation" (Project No. 20034024) and "Soft Matter Physics" (Project No. 21015010).

■ REFERENCES

(1) Schroeder, T. E. *Proc. Natl. Acad. Sci. U.S.A.* **1973**, *70*, 1688–1692.
(2) Albrecht-Buehler, G.; Lancaster, R. M. *J. Cell Biol.* **1976**, *71*, 370–382.
(3) Taylor, D. L.; Condeelis, J. S. *Int. Rev. Cytol.* **1979**, *56*, 57–144.
(4) Byers, H. R.; Fujikawa, K. *J. Cell Biol.* **1982**, *93*, 804–811.
(5) Mitchison, T. J.; Kirschner, M. *Neuron* **1988**, *1*, 761–772.
(6) Mitchison, T. J.; Cramer, L. P. *Cell* **1996**, *84*, 371–379.
(7) Hotani, H.; Inaba, T.; Nomura, F.; Takeda, S.; Takiguchi, K.; Itoh, T. J.; Umeda, T.; Ishijima, A. *Biosystems* **2003**, *71*, 93–100.
(8) Rodriguez, O. C.; Schaefer, A. W.; Mandato, C. A.; Forscher, P.; Bement, W. M.; Waterman-Storer, C. M. *Nat. Cell Biol.* **2003**, *5*, 599–609.
(9) *Giant Vesicles: Perspectives in Supramolecular Chemistry*; Luisi, P. L., Walde, P., Eds.; Wiley: Chichester, U.K, 2000.
(10) Cortese, J. D.; Schwab, B., III; Frieden, C.; Elson, E. L. *Proc. Natl. Acad. Sci. U.S.A.* **1989**, *86*, 5773–5777.
(11) Fygenson, D. K.; Marko, J. F.; Libchaber, A. *Phys. Rev. Lett.* **1997**, *79*, 4497–4500.
(12) Häckl, W.; Bärmann, M.; Sackmann, E. *Phys. Rev. Lett.* **1998**, *80*, 1786–1789.
(13) Limozin, L.; Bärmann, M.; Sackmann, E. *Eur. Phys. J. E* **2003**, *10*, 319–330.
(14) Limozin, L.; Roth, A.; Sackmann, E. *Phys. Rev. Lett.* **2005**, *95*, 178101.
(15) Limozin, L.; Sackmann, E. *Phys. Rev. Lett.* **2002**, *89*, 168103.
(16) Miyata, H.; Hotani, H. *Proc. Natl. Acad. Sci. U.S.A.* **1992**, *89*, 11547–11551.
(17) Miyata, H.; Nishiyama, S.; Akashi, K.; Kinosita, K., Jr. *Proc. Natl. Acad. Sci. U.S.A.* **1999**, *96*, 2048–2053.
(18) Bangham, A. D. *BioEssays* **1995**, *17*, 1081–1088.
(19) Lasic, D. D. In *Structure and Dynamics of Membranes*; Lipowsky, R., Sackmann, E., Eds.; Elsevier Science: Amsterdam, 1995; Vol. 1a, p 491.
(20) De Geest, B. G.; De Koker, S.; Sukhorukov, G. B.; Kreft, O.; Parak, W. J.; Skirtach, A. G.; Demeester, J.; De Smedt, S. C.; Hennink, W. E. *Soft Matter* **2009**, *5*, 282–291.
(21) Pautot, S.; Frisken, B. J.; Weitz, D. A. *Proc. Natl. Acad. Sci. U.S.A.* **2003**, *100*, 10718–10721.
(22) Pautot, S.; Frisken, B. J.; Weitz, D. A. *Langmuir* **2003**, *19*, 2870–2879.
(23) Noireaux, V.; Libchaber, A. *Proc. Natl. Acad. Sci. U.S.A.* **2004**, *101*, 17669–17674.
(24) Yamada, A.; Yamanaka, Y.; Hamada, T.; Hase, M.; Yoshikawa, K.; Baigl, D. *Langmuir* **2006**, *22*, 9824–9828.
(25) Hamada, T.; Miura, Y.; Komatsu, Y.; Kishimoto, Y.; Vestergaard, M.; Takagi, M. *J. Phys. Chem. B* **2008**, *112*, 14678–14681.
(26) Sugiura, S.; Kuroiwa, T.; Kagota, T.; Nakajima, M.; Sato, S.; Mukataka, S.; Walde, P.; Ichikawa, S. *Langmuir* **2008**, *24*, 4581–4588.
(27) Takiguchi, K.; Yamada, A.; Negishi, M.; Tanaka-Takiguchi, Y.; Yoshikawa, K. *Langmuir* **2008**, *24*, 11323–11326.
(28) Pontani, L.-L.; van der Gucht, J.; Salbreux, G.; Heuvingh, J.; Joanny, J.-F.; Sykes, C. *Biophys. J.* **2009**, *96*, 192–198.
(29) Kato, A.; Shindo, E.; Sakaue, T.; Tsuji, A.; Yoshikawa, K. *Biophys. J.* **2009**, *97*, 1678–1686.
(30) Tsuji, A.; Yoshikawa, K. *J. Am. Chem. Soc.* **2010**, *132*, 12464–12471.
(31) Takiguchi, K.; Yamada, A.; Negishi, M.; Honda, M.; Tanaka-Takiguchi, Y.; Yoshikawa, K. *Methods Enzymol.* **2009**, *464*, 31–53.
(32) Janson, L. W.; Kolega, J.; Taylor, D. L. *J. Cell Biol.* **1991**, *114*, 1005–1015.
(33) Pollard, T. D.; Blanchoin, L.; Mullins, R. D. *Annu. Rev. Biophys. Biomol. Struct.* **2000**, *29*, 545–576.
(34) Takiguchi, K. *J. Biochem.* **1991**, *109*, 520–527.
(35) Tanaka-Takiguchi, Y.; Kakei, T.; Tanimura, A.; Takagi, A.; Honda, M.; Hotani, H.; Takiguchi, K. *J. Mol. Biol.* **2004**, *341*, 467–476.
(36) Gibrat, G.; Pastoriza-Gallego, M.; Thiebot, B.; Breton, M.-F.; Auvray, L.; Pelta, J. *J. Phys. Chem. B* **2008**, *112*, 14687–14691.
(37) Langzhou, S. L.; Hobaugh, M. R.; Shustak, C.; Cheley, S.; Bayley, H.; Gouaux, J. E. *Science* **1996**, *274*, 1859–1866.
(38) Okumus, B.; Arslan, S.; Fengler, S. M.; Sua Myong, S.; Ha, T. *J. Am. Chem. Soc.* **2009**, *131*, 14844–14849.
(39) Takiguchi, K.; Hayashi, H.; Kurimoto, E.; Higashi-Fujime, S. *J. Biochem.* **1990**, *107*, 671–679.
(40) Köhler, S.; Lieleg, O.; Bausch, A. R. *PLoS ONE* **2008**, *3*, e2736.
(41) Popp, D.; Akihiro Yamamoto, A.; Iwasa, M.; Maéda, Y. *Biochem. Biophys. Res. Commun.* **2006**, *351*, 348–353.
(42) Suzuki, A.; Yamazaki, M.; Ito, T. *Biochemistry* **1989**, *28*, 6513–6518.
(43) Suzuki, A.; Yamazaki, M.; Ito, T. *Biochemistry* **1996**, *35*, 5238–5244.
(44) Verkhovsky, A. B.; Borisy, G. G. *J. Cell Biol.* **1993**, *123*, 637–652.
(45) Verkhovsky, A. B.; Svitkina, T. M.; Borisy, G. G. *J. Cell Sci.* **1997**, *110*, 1693–1704.
(46) Arai, R.; Mabuchi, I. *J. Cell Sci.* **2002**, *115*, 887–898.
(47) Negishi, M.; Sakaue, T.; Takiguchi, K.; Yoshikawa, K. *Phys. Rev. E* **2010**, *81*, 051921.
(48) Claessens, M. M. A. E.; Tharmann, R.; Kroy, K.; Bausch, A. R. *Nat. Phys.* **2006**, *2*, 186–189.
(49) Kron, S. J.; Toyoshima, Y.; Uyeda, T. Q. P.; Spudich, J. A. *Methods Enzymol.* **1991**, *196*, 399–416.
(50) Nédélec, F. J.; Surrey, T.; Maggs, A. C.; Leibler, S. *Nature* **1997**, *389*, 305–308.
(51) Kruse, K.; Joanny, J. F.; Jülicher, F.; Prost, J.; Sekimoto, K. *Phys. Rev. Lett.* **2004**, *92*, 078101.
(52) Yamaji, K.; Kanai, T.; Nomura, S. M.; Akiyoshi, K.; Negishi, M.; Chen, Y.; Atomi, H.; Yoshikawa, K.; Imanaka, T. *NanoBioscience* **2009**, *8*, 325–331.
(53) Noireaux, V.; Maeda, Y. T.; Libchaber, A. *Proc. Natl. Acad. Sci. U.S.A.* **2011**, *108*, 3473–3480.
(54) Lauffenburger, D. A.; Alan, F.; Horwitz, A. F. *Cell* **1996**, *84*, 359–369.
(55) Popp, D.; Akihiro Yamamoto, A.; Maéda, Y. *J. Mol. Biol.* **2007**, *368*, 365–374.
(56) Pollard, T. D. *Annu. Rev. Biophys. Biomol. Struct.* **2007**, *36*, 451–477.
(57) Pollard, T. D.; Borisy, G. G. *Cell* **2003**, *112*, 453–465.
(58) Murrell, M.; Pontani, L.-L.; Guevorkian, K.; Cuvelier, D.; Nassoy, P.; Sykes, C. *Biophys. J.* **2011**, *100*, 1400–1409.
(59) Foth, B. J.; Goedecke, M. C.; Soldati, D. *Proc. Natl. Acad. Sci. U.S.A.* **2006**, *103*, 3681–3686.